Article

Colorimetric determination of sulfate via an enzyme cascade for high-throughput detection of sulfatase activity

José G. Ortiz-Tena, Broder Rühmann, and Volker Sieber

Anal. Chem., **Just Accepted Manuscript** • DOI: 10.1021/acs.analchem.7b03719 • Publication Date (Web): 08 Jan 2018

Colorimetric determination of sulfate *via* an enzyme cascade for high-throughput detection of sulfatase activity

Jose G. Ortiz-Tena[a], Broder Rühmann[a], Volker Sieber[a,b,c,d*]

[a]Chair of Chemistry of Biogenic Resources, Technische Universität München, Straubing, Germany

[b]Fraunhofer IGB, Straubing Branch BioCat, Straubing, Germany

[c]TUM Catalysis Research Center, Ernst-Otto-Fischer-Straße 1, 85748, Garching, Germany

[d]The University of Queensland, School of Chemistry and Molecular Biosciences, 68 Copper Road, St. Lucia 4072, Australia

*Phone: +49 (9421) 187-300. E-mail: Sieber@tum.de

ABSTRACT: High-throughput screening (HTS) methods have become decisive for the discovery and development of new biocatalysts and their application in numerous fields. Sulfatases, a broad class of biocatalysts that hydrolyze sulfate esters, are involved in diverse relevant cellular functions (e.g., signaling and hormonal regulation) and are therefore gaining importance, particularly in the medical field. Additionally, various technical applications have been recently devised. One of the major challenges in the field of enzyme development is the sensitive and high-throughput detection of the actual product of the biocatalyst of interest without the need for chromophore analogues. Addressing this issue, a colorimetric assay for sulfatases was developed and validated for detecting sulfate through a two-step enzymatic cascade, with a linear detection range of 3.3 (limit of detection) up to 250 µM. The procedure is compatible with relevant compounds employed in sulfatase reactions, including co-solvents, cations, and buffers. The assay was optimized and performed as part of a 96-well screening workflow that included bacterial growth, heterologous sulfatase expression, cell lysis, sulfate ester hydrolysis, inactivation of cell lysate, and colorimetric sulfate determination. With this procedure, the activity of an aryl and an alkyl sulfatase could be confirmed and validated. Overall, this assay provides a simple and fast alternative for screening and engineering sulfatases from DNA libraries (e.g., using metagenomics) with medical or synthetic relevance.

Current advances in enzyme discovery and engineering rely highly on the analytical screening methods used. The decision on how to screen large mutant or metagenomic libraries is a crucial step for the success of any enzyme optimization or search procedure.[1] Microplate assays play a key role in the screening phase because the existing compatible robotics enables fast processing of a large number of enzyme variants. Recently, sulfatases (EC 3.1.6.X) have attracted the interest of various disciplines from the scientific community owing to both their biological relevance and the technical applications devised in different fields.[2] Sulfatases represent a very broad family of enzymes that catalyze the hydrolysis of sulfate esters from a wide spectrum of substrates. These enzymes are involved in numerous cellular functions, such as cell signaling, cellular degradation, hormone regulation, and pathogenesis.[2] As they play an essential role in several diseases, their relevance in human health has been increasingly recognized.[3] Given that the sulfation degree of their substrates is decisive for, e.g., ligand activity (which appears to be strongly related to certain types of cancer[4]), the inhibition and modulation of sulfatases' activity towards signaling molecules have been increasingly studied.[5,6] Furthermore, several technical applications of sulfatases have been developed, such as the enantioselective production of *sec*-alcohols from alkyl sulfates[7] or the regioselective cleavage of sulfate groups from different types of carrageenan to control its gelling or texturizing properties.[8] The increasing importance of this type of biocatalyst is reflected in the recent creation of a sulfatase classification database,[9] which arranges enzymes according to their substrate specificity into alkyl or aryl sulfatases. Given the enormous diversity of sulfated substrates, enzyme HTS procedures are far from being straightforward. The substrates used as standards to detect sulfatases' activity include *p*-nitrophenyl- or *p*-nitrocatechol-sulfate for aryl sulfatases and chromogenic substrate analogues for alkyl sulfatases.[10] For example, a very sensitive sulfatase activity assay was recently proposed in which the fluorescent compound *N*-methylisoindole is produced after sulfatase cleavage of a corresponding sulfated chromophore.[11] However, these assays are only selective for sulfatases that are active on the non-natural substrates that contain such pro-fluorescent probes. Although the easy colorimetric or UV detection of the corresponding de-sulfated products makes their use very convenient, this strategy does not necessarily guarantee activity on the actual substrate of interest, and the analogues are usually expensive. If the de-sulfated product is not chromogenic, instrumental analytical techniques (liquid or gas chromatography, mass spectrometry and nuclear magnetic resonance) are required to detect the hydrolyzed product, which impedes high-throughput processing of large enzyme libraries. Direct sulfate detection would enable the screening and discovery of sulfatases regardless of the substrate type. For a wide range of common food and environmental applications (e.g., sludge or drinking water analyses), sulfate is sensitively detected (0.1 mg L^{-1}) and quantified using ion chromatography or lead ion-selective electrodes.[12,13] Given the long

experimental times, large eluent volumes, and tedious sample preparation associated with such procedures, they are rather unsuitable to realize HTS. Turbidimetric determination of sulfate precipitates with barium chloride has become the method of choice when large amounts of samples are measured because the procedure is straightforward and compatible with the microplate format. Several variants of this method have been developed for different applications, e.g., bacterial cultures,[14] human urine,[15] or industrial effluents,[16] and commercial kits are readily available. However, the precipitation of barium sulfate for generating a turbidimetric signal is strongly dependent on multiple factors, e.g., suspension stabilizing reagent used, ionic strength of the sample, and protein concentration.[14] Therefore, the application of turbidimetry using barium chloride for screening sulfatases from cell lysates is somewhat inappropriate; as organic components, such as glycosaminoglycans and peptides strongly inhibit the precipitation of $BaSO_4$.[17] Recently, a study on a sensitive colorimetric assay for sulfate detection was published in which cysteamine-coated gold nanoparticles aggregated in the presence of SO_4^{2-} ions, inducing a detectable absorption shift in the range of 0.34–30 µM, with a sigmoidal sulfate calibration curve.[18] Also, highly sensitive phosphatase assays have been recently developed based on the application of various nanostructures. The output signal of these methods, which in part involve substrate-coordinated compounds, ranges from colorimetry to fluorescence and voltammetry. Unfortunately, their utilization for the analysis of sulfatases has not been shown.[19-21] In this study, addressing the need for a reliable, sensitive, and inexpensive alternative for screening sulfatase libraries with a broad detection range, a colorimetric assay was developed and validated for sulfate determination based on a two-step enzymatic cascade. After optimizing the relevant reaction parameters of the enzymatic cascade, the assay was validated and the influence thereon of pertinent compounds was evaluated. Sample preparation was then adjusted for optimal sulfate detection in bacterial lysates and the application of the assay for HTS of sulfatase activity was demonstrated by determining the activity of heterologously expressed aryl and alkyl sulfatases in *E. coli* in microplate format.

EXPERIMENTAL SECTION

Chemicals and enzymes: All chemicals were of analytical grade and were purchased from Sigma Aldrich, Merck KGaA, and Carl Roth GmbH. Pyruvate oxidase (POX) and horseradish peroxidase (HRP) were obtained from Sigma Aldrich. The leuco dye N-(carboxymethylaminocarbonyl)-4,4′-bis(dimethylamino)diphenylaminesodium salt (DA-64) was acquired from Wako. The genes for pyruvate phosphate dikinase from *Propionibacterium freudenreichii* (PPDK) and APS kinase (APSk) from *S. cerevisiae* were purchased from Genscript in pET-28a(+) expression vectors; they were heterologously produced in *E. coli* BL21 DE3 and purified using affinity chromatography according to published protocols.[22,23] The *cysDN* gene encoding ATP sulfurylase (ATPs) with GTPase activity was amplified from *E. coli* genomic DNA using designed primers (see supplementary information), cloned into pET-28a(+), and purified *via* affinity chromatography with a Ni-NTA column (Aekta, GE). Aryl sulfatase from *P. aeruginosa* (PAS) and alkyl sulfatase from *Pseudomonas sp.* DSM6611 (PISA1) were purified as previously described.[7,24] The concentrations of the purified enzymes were determined using a nanophotometer (Implen, P-330) by employing the parameters from the online tool ProtParam (SIB, Switzerland; Table S1). All purified enzymes and assay reactants were aliquoted, stored at −20 °C and used only once. 2-heptyl sulfate (PISA1 substrate) was synthesized as previously described[25] with modifications (see supplementary material).

Assay optimization: The colorimetric assay was subsequently optimized by evaluating a K_2SO_4 calibration curve constructed in the range 2.5–250 µM. Since reaction 2 of the assay (Scheme 1) is already established for determining pyrophosphate and pyruvate,[22,26] the optimization was focused on reaction 1 and each optimization round served as basis for the next. Optimization reactions were performed in duplicate by mixing 50 µL of K_2SO_4 standard and 50 µL of master mix 1. After incubation at 25 °C for varying times depending on the optimization round (see below), 100 µL of master mix 2 (K_2HPO_4 100 mM pH 6.5, DA-64 100 µM, thiamine pyrophosphate (TPP) 50 µM, $MgCl_2$ 100 µM, phosphoenolpyruvate (PEP) 500 µM, adenosine monophosphate (AMP) 500 µM, PPDK 50 mU, POX 50 mU, and HRP 200 mU; concentrations in reaction) was added to the abovementioned solution. The mixture was then incubated at 37 °C for 30 min. In all cases, the absorbance (A) was measured at 727 and 540 nm (Varioskan, Thermo Scientific), and $A_{727-540}$ was computed for each standard and a sulfate blank. The calibration curve was then calculated by subtracting the sulfate blank absorbance value from each calibration point ($\Delta A_{727-540}$). The first optimization round focused on finding the best enzymatic concentrations for reaction 1 in HEPES (4-2-hydroxyethyl-1-piperazineethanesulfonic acid) 12.5 mM pH 7.8, GTP 2 mM, ATP 1 mM, and $MgCl_2$ 3 mM (final concentrations, incubation time 45 min). Next, GTP and ATP concentrations were varied (HEPES 12.5 mM pH 7.8, $MgCl_2$ 3 mM, ATPs 0.46 µM, and APSk 5.3 µM; final concentrations, incubation time 45 min). The optimal reaction time was determined from four equal intervals between 15 and 90 min using the previously found optimal concentrations (HEPES 12.5 mM pH 7.8, GTP and ATP 1 mM, $MgCl_2$ 3 mM, ATPs 0.46 µM, and APSk 5.3 µM, concentrations in reaction).

Assay validation and characterization: All the data obtained were verified for normal distribution *via* standard skewness and kurtosis tests. For intra-day repeatability and inter-day reproducibility validation, the standard deviation (SD) and precision were calculated using the Student's *t*-test (P = 95%, n = 4 and 6, respectively). The limit of detection (LOD) was calculated as $b \pm 3\sigma_{Blank}$ and the limit of quantification (LOQ) was $b \pm 10\sigma_{Blank}$, where b is the y-intercept of the calibration curve. The effect of 100, 50, and 25 mM HEPES, TRIS (2-amino-2-(hydroxymethyl) propane-1,3-diol), MOPS (3-morpholinopropane-1-sulfonic acid), citrate, and phosphate buffers at the corresponding pK_a was evaluated by first spiking the samples with a K_2SO_4 solution (100 µM) and then adding the buffers to a complete calibration curve. The influence of various metal ions at different concentrations (1.0, 0.1, and 0.01 mM) was also investigated by spiking with 100 µM K_2SO_4 solutions and calculating the recovery. Different solvents at 5% v/v (final concentration in assay) were spiked with 100 µM sulfate as well.

Assay application in sulfatase reactions: First, the applicability of the developed assay for screening sulfatase activity was assessed using purified PAS and PISA1. The reaction for PAS (3.0 nM) was performed using *p*-nitrophenyl sulfate (250 µM) as the model substrate in TRIS 100 mM (pH 8, 1 mL reaction volume) at 30 °C overnight. The concentration of *p*-nitrophenol produced was determined from the absorbance at 400 nm, quantifying against a standard calibration

curve. The reaction for PISA1 (1.8 µM) was performed with 2-heptyl-sulfate as previously described.[27] The concentration of sulfate released by both enzymes was quantified using the optimized colorimetric assay.

The influence of different cell lysis methods on the assay was tested. For this, *E. coli* BL21 DE3 bearing the pET-28a(+) empty vector were cultured overnight at 37 °C. The cells were centrifuged and re-suspended in HEPES (100 mM, pH 8) containing either B-Per™ (Thermo Scientific) or Bug-Buster® (Merck) according to manufacturer's instructions, lysozyme (2.5 mg mL^{-1}), and DNase (10 µg mL^{-1}). The cells were incubated for 1 h at 37 °C, and the sulfate content was measured in spiked dilutions prior to and after a 5-min incubation step at 70 °C. In a second experiment, different inactivation times were evaluated over the whole calibration range. As large signal variability was observed in bacterial lysates with encoding sulfatases, the stabilizing effect of bovine serum albumin (BSA) at different concentrations in the lysis solution was evaluated.

Sulfatase screening procedure: *E. coli* BL21 DE3 colonies bearing the expression vectors pASK-IBA5+_PAS, and pET-21(+)_PISA1 and a corresponding empty vector were picked from lysogeny broth (LB) agar plates (RapidPick CP-7200, Hudson). The colonies were then inoculated into a pre-culture deep well plate (Greiner) containing 1.2 mL of LB medium with carbenicillin (100 µg mL^{-1}) and grown at 37 °C overnight. 20 µL of the pre-culture was then used to inoculate an expression plate, and the cells were incubated for 2 h at 37 °C. The expression of PAS was induced with anhydrotetracycline (200 µg L^{-1}) at 30 °C for 2 h.[7] The PISA1-bearing cells were induced with IPTG (0.5 mM), expression conducted at 20 °C for 10 h.[28] After collecting the cell pellet by centrifugation (3000 g, 15 min), 500 µL of lysis solution containing HEPES 100 mM, Bugbuster® protein extraction reagent (according to manufacturers' instructions), lysozyme (2.5 mg mL^{-1}), DNase (10 µg mL^{-1}), and BSA (2.5 g L^{-1}) was added to each well, and the plate was incubated for 1 h at 37 °C and 1000 rpm. After centrifugation of cell debris (4000 g, 15 min), 450 µL of cell lysates were transferred to a new U-bottom plate (Riplate, Ritter) and incubated at the respective T_{opt} for each sulfatase (57 °C and 1 h for PAS $c_{pNP\text{-}Sulfate}$ = 1 mM[29] and 25 °C and 10 h for PISA1 $c_{2\text{-}heptyl\text{-}Sulfate}$ = 5 mM). At the end of the reaction, cell lysates were inactivated in a water bath at 70 °C for 30 min. The concentration of the *p*-nitrophenol produced by PAS was determined at 400 nm and quantified against a standard calibration curve in micro titer plates (Greiner) using a 20-µL sample. The content of the sulfate released by both enzymes was quantified using the optimized assay with 5-µL samples.

Optimized assay: The final assay was performed by mixing 50 µL of the sample or standard with 50 µL of master mix 1 (HEPES 12.5 mM pH 7.8, GTP and ATP 1 mM, $MgCl_2$ 3 mM, ATPs 0.46 µM, APSk 5.3 µM). An incubation step at 25 °C for 45 min followed and then 100 µL of master mix 2 was added (K_2HPO_4 100 mM pH 6.5, DA-64 100 µM, TPP 50 µM, $MgCl_2$ 100 µM, PEP 500 µM, AMP 500 µM, PPDK 50 mU, POX 50 mU, HRP 200 mU). The plate was then incubated for 30 min at 37 °C and $A_{727-540}$ was computed.

RESULTS AND DISCUSSION

For any assay aiming to identify an analyte of interest, a recognition element is required in the detection system, followed by a transducer element, e.g., colorimetric signal, whose intensity correlates to the analyte' s concentration. Owing to their outstanding specificity, enzymes offer unique advantages as molecular recognition elements in analytical chemistry.[30] As sulfate ion is the analyte of interest in this case, an enzyme that utilizes it as a substrate is required as the recognition element. However, the unreactive nature of sulfate makes the selection of this enzyme challenging. ATP sulfurylase (ATPs, EC 2.7.7.4) catalyzes the universal starting step in the sulfur metabolism *in vivo*, "activating" SO_4^{2-} by transferring it to adenosine triphosphate (ATP) through a highly endergonic reaction ($\Delta G^{o\prime}$ = 19.5 kcal mol^{-1}).[31] Adenosine-5′-phosphosulfate (APS) and inorganic pyrophosphate (PP_i) are formed as the products in a reaction whose equilibrium favors the reactant side ($K = 10^{-8}$).[32] This issue is solved *in vivo* by many organisms through channeling complexes, in which APS is immediately transferred from the active site of the ATPs to an embedded APS kinase (APSk, EC 2.7.1.25), which in turn phosphorylates APS, shifting the equilibrium to the product side.[33] A promising alternative for performing this reaction *in vitro*, without the need of such a complex, is the ATPs/GTPase from *E. coli*.[34] This enzyme can couple the chemical potential of guanosine triphosphate (GTP) hydrolysis with the unfavorable activation of sulfate to produce APS, PP_i, and GDP. This particular feature is not displayed by ATPs from other organisms, e.g., *S. cerevisiae*.[35] Given this advantage, the ATPs/GTPase reaction was selected as the starting step of the proposed cascade for sulfate detection (Scheme 1). This reaction can be further driven towards completion by the immediate phosphorylation of APS to afford 3′-phosphoadenosine 5′-phosphosulfate (PAPS) using APSk from *S. cerevisiae*. Of all the products formed to this point, the resulting equimolar production of PP_i from sulfate enables the possibility of connection to a transducer element. Its detection is possible owing to a second set of enzyme-catalyzed reactions, which rely on the previously described assays for amino acids based on PP_i detection using pyruvate phosphate dikinase (PPDK) from *Propionibacterium freudenreichii*.[36] The PP_i released by ATPs/GTPase reacts with adenosine monophosphate (AMP) and phosphoenolpyruvate (PEP) to produce pyruvate, which is in turn oxidized by pyruvate oxidase (POX) to afford H_2O_2. In the last reaction of the cascade, horseradish peroxidase (HRP) catalyzes the oxidation of the dye DA-64 to produce Bindschedler's green using the H_2O_2 produced, yielding a colorimetric signal at 727 nm, which is proportional to the sulfate concentration in the sample. The measurement at this particular wavelength avoids detection in the yellow region of the spectra, in which several disturbing compounds or matrices exhibit absorbance (e.g., bacterial culture media or aromatic compounds).

Scheme 1. Enzymatic cascade for colorimetric detection of inorganic sulfate.

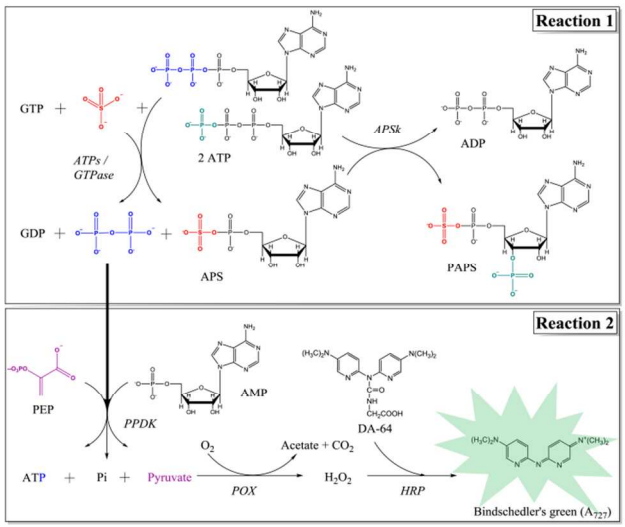

ATPs: ATP sulfurylase; *APSk*: APS kinase; *PPDK*: pyruvate phosphate dikinase; *POX*: pyruvate oxidase; *HRP*: horseradish peroxidase; DA-64: N-(carboxymethylaminocarbonyl)-4,4′-bis (dimethylamino) diphenylaminesodium. The equilibrium of the two reactions lies strongly on the product side.

Assay optimization: Owing to the complexity of the reaction cascade, a number of variables need to be explored for the assay to achieve good linearity and reproducibility over the intended detection range. Most importantly, note that the reaction parameters are not compatible for all the enzymes. ATPs/GTPase and APSk act optimally at pH ~8 and 25 °C, while the optimal conditions for the reaction cascade for detecting PP_i are pH 6.5 and 37 °C; therefore, a change of buffer is necessary. Since determination of PP_i is already a well-established procedure,[36] the optimization focused on the first reaction. The concentration and ratio of enzymes employed in analytical assays are parameters relevant for their robustness. In this case, the molar ratio of ATPs and APSk was set to ~1:10 so that virtually every APS produced by ATPs is immediately converted to PAPS by APSk. The concentration of these enzymes was varied as shown in Fig. S1-A. 0.46 µM ATPs and 5.3 µM APSk were selected because higher and lower concentrations led to lower signals with 250 µM sulfate, decreasing the assay linearity. Next, different GTP and ATP concentrations were explored. This parameter is very important for initiating the ATPs reaction. Ideally, a GTP:ATP molar ratio of 1:2 is expected to generate a steady flowing cascade as 2 ATP molecules are needed in the first reaction: one producing APS and the other for APS phosphorylation to yield PAPS with GDP as the byproduct. However, the accumulation of GDP in the system decreases the ATPs efficiency for coupling GTP hydrolysis to APS synthesis and PP_i release, as competitive inhibition of the guanine nucleotide binding site occurs between GDP and GTP.[37] Accordingly, the concentration of GTP needed to direct the reaction towards SO_4^{2-} consumption must be increased and was, therefore, set to at least a 1:1 GTP:ATP molar ratio. The GTP and ATP concentration that best fitted the curve in the desired calibration range was 1 mM (Fig. S1-B). By setting a higher GTP concentration (2 mM), the linearity of the assay decreases in the low-concentration range. Lastly, different times for reaction 1 were tested (Fig. S1-C). The sensitivity of the calibration curve increased as reaction time increased (15, 30, and 45 min) and then decreased again at 60 and 90 min. Too-short times may not be adequate for the complete reaction of sulfate, especially at the higher concentrations in the calibration curve. On the other hand, too-long times might shift the equilibrium back to the production of ATP and SO_4^{2-}, as previously described for the ATPs reaction.[37] Thus, a reaction time of 45 min was considered optimal and employed. As a result of the optimization procedure, a linear calibration curve was obtained: $y = 0.0057x + 0.0194$ with $R^2 = 0.9983$, in the range 5.0–250 µM SO_4^{2-}. The sulfate blank of the calibration curve in water presented a moderate $A_{727-540}$ value of ~0.32 in deep well plates ($V_{sample} = 200$ µL), which was attributed to auto hydrolysis of the nucleotides to form PP_i, ATPs-catalyzed non-sulfate-dependent hydrolysis of ATP to yield PP_i and AMP, and PEP degradation to produce pyruvate and phosphate over the course of reaction 2.

Assay validation and characterization: After confirming the normal distribution of the data using the standard skewness and kurtosis tests, validation analysis was performed. The calculated LOD and the LOQ were 3.3 µM and 10.9 µM, respectively. It is worth noting that commercial turbidimetric assays with barium chloride allow a detection limit of 5 mg L^{-1} (52 µM),[38] while the previously reported sulfate assay using gold nanoparticles exhibited a LOD of 0.34 µM, allowing quantification up to 30 µM with a sigmoidal response curve.[18] The present assay allows linear measurement of a broader range, which renders it more sensitive over the whole calibration range. The SD, precision, and accuracy for determining the intra-day repeatability and inter-day reproducibility are shown in Table 1. The precision, as calculated by the Student's *t*-test (P = 95%), ranges from 1% for 250 µM sulfate to 15% near the LOQ, while the accuracy bias varies from −1% for the highest calibration point to 23% around the LOQ. These results are similar to those reported for the gold nanoparticle method and ion chromatography for real samples (> 95% accuracy for samples spiked with 25 and 50 ppm sulfate)[18] and indicate an excellent performance in the upper working range that tends to decrease at sulfate concentrations lower than 25 µM.

Table 1. Analytical performance of the proposed assay

SO_4^{2-} µM	Intra-day Repeatability			
	Mean µM	SD	Precision[a]	Accuracy Bias[a]
250	247	2.0	1.3%	-1.2%
100	106	3.0	4.5%	6.6%
25	24.3	1.8	11.9%	-2.9%
10	7.7	0.7	14.6%	-23%
SO_4^{2-} µM	Inter-day Reproducibility			
	Mean µM	SD	Precision[b]	Accuracy Bias[b]
250	247	0.5	0.2%	-1.1%
100	106	1.5	1.5%	6.3%
25	23.8	1.1	4.7%	-4.9%
10	7.8	0.4	5.6%	-22%

Calculated using the Student's *t*-test with [a]n = 4, [b]n = 6.

The influence of commonly employed compounds in sulfatase reactions was also evaluated on the enzymatic assay. First, the detection of 100 µM sulfate was assessed in the presence of different buffers (25, 50, and 100 mM, Fig. 1A). Citrate buffer at the tested concentrations was not compatible with the assay as no signal was detected. The recovery of sulfate in MOPS increased from 65% at 100 mM to 81% at 25 mM. The phosphate buffer had the most considerable effect at different concentrations, with recoveries ranging from 56 to 128%. TRIS and HEPES afforded the best sulfate recoveries, 86–105%, at the tested concentrations. To investigate whether the observed effect was dependent on sulfate concentration, calibration curves containing the buffers were analyzed (Fig. S2-A). An absorption signal lower than that of

pure water was observed in samples containing 100 mM MOPS, TRIS, and HEPES over the whole calibration range; its effect in the quantification may be hence compensated by preparing the calibration curve in these buffers or by diluting the samples to improve recovery. Conversely, the phosphate buffer has a great impact in the assay, as the absorption values of the sulfate blank at 100 mM and 25 mM were higher than that for the abovementioned buffers and nearly no sulfate-dependent increase in absorbance was detected. A more pronounced slope was evident in the calibration curve at concentrations between 0.5 and 2.0 mM phosphate with $A_{727-540}$ signals higher than that for the curve prepared in water. This effect could lead to false positive results (Fig. S2-B). Considering that reaction 2 occurs in a phosphate buffer, it is likely that phosphate has a great effect on reaction 1 at low sulfate concentrations. This suggests that competitive inhibition between phosphate and sulfate may occur in the active site of ATPs, causing a non-sulfate-dependent release of PP_i, thus producing the higher signals observed. Therefore, it is not recommended to perform the assay when samples contain phosphate at concentrations exceeding 0.1 mM (Fig. S2-B). This limitation should be considered when preparing sulfatase samples.

Organic solvents are commonly employed in sulfatase reactions at 20% v/v to solubilize hydrophobic sulfated substrates and to increase the selectivity of some sulfatases.[10] Therefore, the tolerance of the assay towards different solvents at 5% v/v was tested (Fig. 1B). Ethanol, methanol, DMF, and DMSO exhibited good compatibility with the assay, with recoveries of 100 ± 10% for 100 µM sulfate. Accordingly, samples containing these organic solvents could be measured after dilution by a factor of 4. With a concentration of sulfated substrates of 1 mM, sulfatase activities between 10%–100% could be easily detected. Moreover, metal ions play an important role in some sulfatase reactions, acting as activators[2] (e.g., Ca^{2+} at 1–5 mM) and inhibitors (e.g., Zn^{2+} at 1 mM) and even influencing the hydrolysis enantioselectivity of *sec*-alkyl sulfates (Fe^{2+} and Co^{2+} at 1–10 mM).[39,40] The determination of 100 µM sulfate was thus evaluated in the presence of various cations at different concentrations (Fig. S3). Ni^{2+}, Zn^{2+}, and Cu^{2+} enable good detection at ≤ 0.01 mM; Fe^{2+} at 0.1 mM (~75% recovery); Co^{2+} and Rb^{+} at ≤ 1 mM, and Ca^{2+} even at 5 mM. Nickel, zinc, and cupper are frequently present in bacterial cultures as trace elements at concentrations between 0.1 and 0.5 mM. Owing to the low tolerance of the assay to iron, a removal strategy, e.g., precipitation may be necessary to perform the assay at concentrations higher than 0.1 mM. Overall, the cation concentration can be adjusted by diluting the samples according to each case.

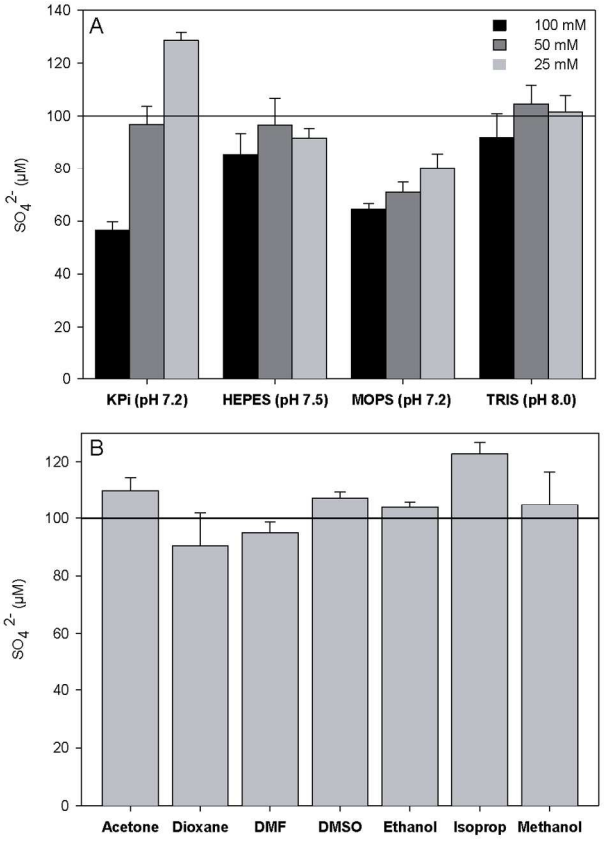

Figure 1. Sulfate determination in the presence of various compounds commonly employed in sulfatase reactions. The solid line indicates the amount of sulfate spiked. A. Buffers at different concentrations. B. Organic solvents at 5% (v/v, assay concentration).

Assay application in sulfatase reactions: After evaluating the performance of the optimized sulfate assay, determination of the enzymatic activity was tested using the aryl sulfatase from *P. aeruginosa* (PAS). This enzyme catalyzes the hydrolysis of *p*-nitrophenyl sulfate, the model substrate for the screening of sulfatases. This reaction generates free sulfate and *p*-nitrophenol, a chromophoric product that can be readily detected at 400 nm in alkaline media. Accordingly, a parallel photometric determination of both products at well-separated wavelengths of the visible spectrum is possible after performing the optimized sulfate assay. The initial substrate concentration was set to 250 µM; after the reaction, 203 µM *p*-nitrophenol (82% conversion) and 188 µM sulfate (75% conversion) were quantified, indicating an accuracy bias of –7% between both determination methods. The absorption spectrum of the reaction containing both products after performing the sulfate assay (Fig. 2, solid line) reveals two peaks: one at 400 nm, corresponding to *p*-nitrophenol (A_{400} = 0.53, l = 1 cm) and another more intense peak at 727 nm resulting from the enzymatic conversion of sulfate to Bindschedler's green through the cascade (A_{727} = 2.61, l = 1 cm). When the substrate is absent (Fig. 2, dashed line), no peak is observed at 400 nm and the intensity of the peak at 727 nm decreases (A_{727} = 0.70, l = 1 cm), as was observed for the sulfate blank in the calibration curve. Under these conditions, a molar extinction coefficient of 10 160 M^{-1} cm^{-1} was calculated for Bindschedler's green, which is directly related to the concentration of sulfate. This coefficient is four times higher than that of *p*-nitrophenol (2 611 M^{-1} cm^{-1}), rendering sulfate colorimetric detection more sensitive than the deter-

mination of *p*-nitrophenol under the sulfatase reaction conditions. For aryl sulfatases, the cleavage of the sulfate ester bond is initiated by a nucleophilic attack of the sulfur atom. However, there are also sulfatases acting on alkyl sulfates, where the ester cleavage is achieved by nucleophilic substitution at the carbon atom (Fig. S4). Such enzymes exhibit no activity with *p*-nitrophenyl sulfate and cannot be assayed as easily as aryl sulfatases. To demonstrate the detection of sulfate released from alkyl sulfatases, in which no chromogenic substrate is involved, PISA1 was purified and its activity was tested towards *rac*-2-heptyl-sulfate. The initial substrate concentration was set to 22 mM.[28] The measured sulfate concentration after a proper dilution was 9.9 mM. This represents an enzymatic conversion of 45% as previously reported; it is worth recalling the high enantioselectivity of PISA1 (E > 200) towards *R*-2-heptyl-sulfate.[28]

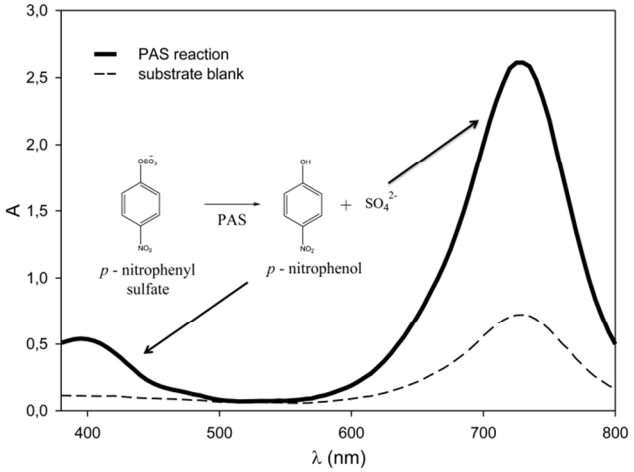

Figure 2. Spectra of the reaction of P. aeruginosa arylsulfatase (PAS) on p-nitrophenyl sulfate measured in cuvettes, l = 1 cm. Reactions performed overnight in TRIS 100 mM, pH 8 at 57 °C.

Sulfatase screening procedure: As the screening and engineering of enzymes is conducted in bacterial lysates of expression strains, the assay was applied for quantifying sulfate in cell lysates in order to evaluate and correct potential matrix effects. The most common method for disrupting bacterial cells is the use of detergents that solubilize the cell membrane in combination with hydrolytic enzymes, such as lysozyme and DNase. First, the determination of spiked sulfate was conducted in various dilutions of cell lysates produced with the two commercially available detergents B-Per™ and Bug-Buster® (Fig. S5-A). The spiked sulfate could not be detected in 1:10 and 1:50 dilutions, and a poor recovery of 50% was obtained at 1:100. This suggests that the surfactant compounds of the lysis solution and the released cell components interfere with the assay either by inhibiting or denaturing the enzymes involved or by interacting with the intermediates (Scheme 1). In order to precipitate potentially interfering *E. coli* proteins, the cell lysates were incubated at 70 °C for 5 min. Afterwards, nearly 100% of sulfate recovery (100 µM) was reached at 1:50 and 1:100 dilutions, but only 50%–60% was reached at 1:10. When increasing the incubation time to at least 20 min in 1.5-mL tubes (Fig. S5-B) and 30 min in 96-deep well plates (data not shown), the detection of sulfate in 1:10 diluted cell lysates was possible over the whole calibration range.

The experiments mentioned above were performed with *E. coli* cells bearing a pET-28a(+) empty plasmid. However, large signal variability was observed when vectors encoding sulfatases were used (data not shown). In such cases, the matrix effects influencing enzymatic assays are difficult to predict, and it was assumed that this resulted from varying cell metabolism or intracellular protein concentrations. Therefore, the protein content of *E. coli* cell lysates bearing the pASK_PAS plasmid was normalized by adding bovine serum albumin (BSA) at different concentrations, spiked with sulfate, and then inactivated at 70 °C for 30 min. BSA significantly improved the detection of sulfate in the cell lysates with expressed sulfatases over the whole calibration range at concentrations above 1 g L^{-1}, with the best linearity at 2.5 g L^{-1} BSA (Fig. 3). The samples were analyzed by gel electrophoresis before and after incubation at 70 °C (Fig. S6), and the presence of BSA was confirmed in the incubated samples containing at least 1 g L^{-1} BSA. Although the thermostabilizing effect of BSA towards enzymes has been described previously,[41] it is not fully clear whether its presence facilitates the thermal precipitation of disturbing *E. coli* components or if it stabilizes the assay enzymes.

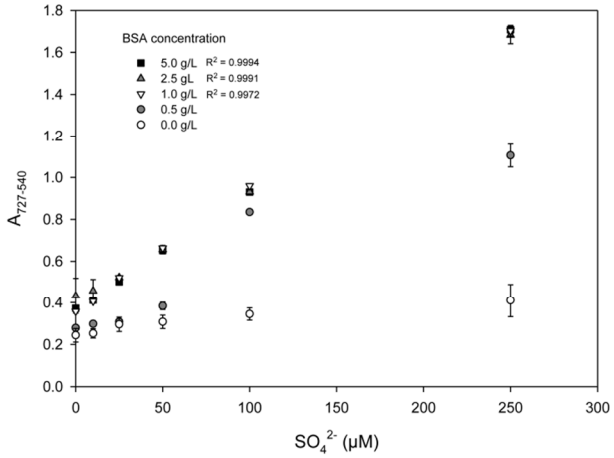

Figure 3. Sulfate calibration curve in cell lysates of *E. coli* bearing pASK_PAS plasmid containing BSA at different concentrations.

Once the optimal conditions for sulfate detection in bacterial lysates were established, a 96-well workflow was designed to create a wild-type landscape of PAS and PISA1 with their respective substrates. While PISA1 has no activity with the chromophore containing *p*-nitrophenyl sulfate, the detection of the sulfate released by the PAS clones can be cross-validated by quantifying *p*-nitrophenol as described above. Figure 4 shows the absorption signals of the products released by both enzymes. The volumes used for each product (20 µL *p*-nitrophenol and 5 µL sulfate) were chosen so that the signals would fit in the corresponding calibration curve. Black dots indicate *E. coli* sulfatase clones and white circles represent empty vector clones (pASK-IBA5+). The output signal $A_{727–540}$ obtained using the assay was 0.82 ± 0.05 (Fig. 4A-2), which was quantified as 0.97 mM $SO_4^{2–}$, while the A_{400} signal for *p*-nitrophenol obtained was 0.97 ± 0.07 (Fig. 4A-1), resulting in a concentration of 0.95 mM, which represents a 2% bias compared to sulfate. This reflects a conversion of ca. 96% under the screening conditions, considering that the initial concentration of *p*-nitrophenyl sulfate was 1 mM. The absorbance values for the negative controls of both procedures were 0.32 ± 0.02 for the sulfate assay and 0.08 ± 0.02 for *p*-nitrophenol.

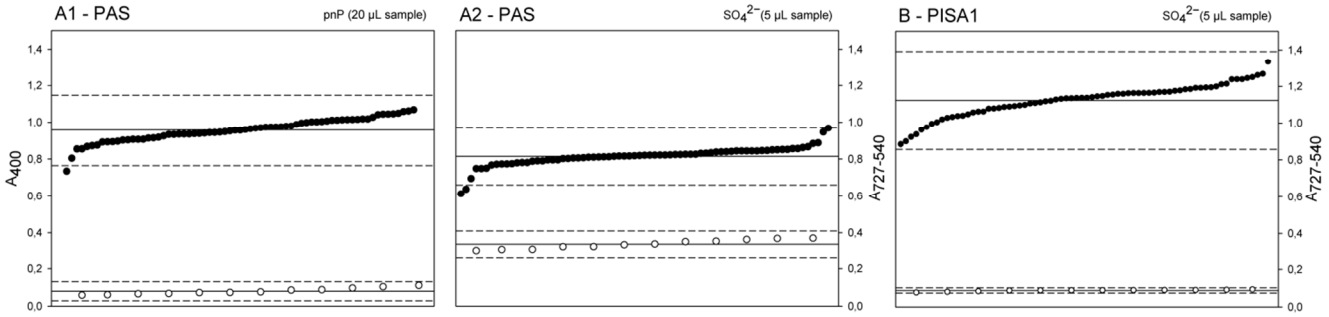

Figure 4. Absorption signals of sulfatase products. A1. pnP: *p*-nitrophenol (400 nm). A2. Sulfate (727–540 nm) from PAS. B. Sulfate (727–540 nm) from PISA1 ●: Positive clones. ○: Empty vector clones. Solid line: mean (μ); dashed lines μ±3σ (standard deviation).

A relevant parameter for the qualitative evaluation of HTS assays is the Z' factor.[42] This dimensionless number evaluates the ability of an assay to discern active clones from inactive ones with high fidelity by computing the signal difference between positive and negative controls in relation to the sum of their standard deviations (noise) and is given by the following equation:

Eqn. (1) $$Z' = 1 - \frac{(3\sigma_{c+} + 3\sigma_{c-})}{|\mu_{c+} - \mu_{c-}|}$$

where μ is the mean and σ the standard deviation of the signals from positive (c+) and empty vector clones (c–). HT assays with a Z' factor of 1 are considered ideal; for assays where $1 > Z' \geq 0.5$, the separation band between positive and negative clones is considered large and the assay provides reliable screening conditions. However, if $Z' < 0.5$, the separation band is small and the assay is considered as a double assay; therefore, it is non-practical for distinguishing positive clones from negative ones with high precision. The detection of *p*-nitrophenol at 400 nm under the presented conditions yielded an excellent Z' value, 0.71, which results from a large signal difference between positive and negative clones. Furthermore, a value of $Z' = 0.51$ was obtained for the colorimetric detection of sulfate, as the separation band between positive and negative clones in this case is smaller than that for *p*-nitrophenol. This value reflects the suitability of the assay for screening aryl sulfatases *via* the detection of sulfate in the calibration range with a very good correlation with the determination of *p*-nitrophenol. As the volume used for *p*-nitrophenol was four times higher than that for sulfate (see above), the two Z' values cannot be compared to each other. The assay user can choose an appropriate sample volume depending on a desired threshold for the reaction yield of positive clones.

The potential of the assay developed becomes evident when such a screening workflow is applied to alkyl sulfatases, e.g., PISA1, as chromogenic substrates are hardly available and do not actually reflect the activity on the compound of interest (Fig. 4B). The output sulfate signal $A_{727–540}$ with this enzyme towards *rac*-2-heptyl-sulfate was 1.12 ± 0.09 for positive clones and 0.09 ± 0.00 for empty vector clones. The amount of sulfate released was 1.8 mM, indicating 36% of conversion from a maximum of 50% enantioselective yield (initial substrate concentration, 5 mM). As the clones bearing the empty vector pET-21+ displayed lower absorbance ($A_{727–540} = 0.09$) than those used in the PAS screening ($A_{727–540} = 0.32$), a broader separation band between positive and negative clones enabled better assay performance, as indicated by $Z' = 0.73$. The lower values obtained with different empty vectors may result from differing induction and growing cell conditions for PAS and PISA1, e.g., anhydrotetracycline *vs* IPTG or the addition of zinc in the PISA1 culture. These results demonstrate the efficacy of the assay for discovering new sulfatases at the DNA level by, e.g., using metagenomic libraries. With this assay, one can avoid the tedious and time-consuming screening of novel sulfatase activity at the protein level in which a large amount of microorganism, plant, or animal cells have to be cultured and numerous extraction and drying steps have to be executed to detect de-sulfated products *via* chromatography, as was the case for the *de novo* discovery of PISA1.[43]

CONCLUSIONS

In this study, a colorimetric assay for detecting sulfate based on a two-step enzymatic cascade was designed, optimized, and experimentally validated. The linearity of the assay in the range 10–250 μM renders it comparable to chromatographic methods in terms of sensitivity (LOD = 3.3 μM sulfate) and superior to established plate procedures such as barium sulfate precipitation or utilization of chromogenic substrates. The proposed method demonstrated good precision and accuracy. Sulfate determination was possible in the presence of pertinent buffers, organic solvents, and metal ions at concentrations relevant for sulfatase reactions. A significant advantage of this assay is its feasibility for screening sulfatase activity in cell lysates, as optimized and demonstrated here for aryl and alkyl sulfatases in an automatable 96-well workflow. The assay showed a very good stability in such a plate workflow ($Z' > 0.5$). Further, the enzymes employed in the assay were still active 3 months after purification when stored at −20 °C. The assay provides a reliable alternative for sulfate analysis and sulfatase activity screening regardless of the substrate type and without the need for chromophore derivatives. The procedure presented herein can be employed for the HTS of large variant libraries (e.g., from mutagenesis or metagenomes). In addition, the assay might also be considered for the general determination of sulfate in different types of samples such as drinking water, bacterial and algal cultures, blood or urine, for which high throughput is of advantage.

ASSOCIATED CONTENT

Supporting Information

Additional information regarding enzyme production and purification, as well as assay optimization and sample adjusting to cell lysates is available as noted in the text. This material can be accessed free of charge on the ACS Publications website at DOI: XXX.

AUTHOR INFORMATION

Corresponding Author

*Phone: +49 (9421) 187-300. E-mail: Sieber@tum.de

Author Contributions

The manuscript was written through contributions of all authors.

Notes

The authors declare no competing financial interests.

ACKNOWLEDGMENTS

The project was founded by the German Federal Ministry of Education and Research, Project ABV 03SF0446A. Special gratitude is expressed to Kurt Faber, Michael Tösch, and Tamara Reiter (TU Graz, Austria) for providing the PAS and PISA1 genes. The authors are extremely thankful to Dr. Josef Sperl for assisting with the amplification and cloning of *cysDN* and to Petra Lommes for conducting the synthesis of 2-heptyl-sulfate.

REFERENCES

(1) Bloom, J. D.; Meyer, M. M.; Meinhold, P.; Otey, C. R.; MacMillan, D.; Arnold, F. H. *Curr Opin Struc. Biol.* **2005**, *15*, 447–452.
(2) Hanson, S. R.; Best, M. D.; Wong, C. H. *Angew. Chem.-Int. Edit.* **2004**, 5736–5763.
(3) Diez-Roux, G.; Ballabio, A. *Annu. Rev. Genom. Hum. G.* **2005**, *6*, 355–379.
(4) Vivès, R. R.; Seffouh, A.; Lortat-Jacob, H. *Front. Oncol.* **2014**, *3*, 1-11.
(5) Schelwies, M.; Brinson, D.; Otsuki, S.; Hong, Y. H.; Lotz, M. K.; Wong, C. H.; Hanson, S. R. *ChemBioChem* **2010**, *11*, 2393–2397.
(6) Reuillon, T.; Alhasan, S. F.; Beale, G. S.; Bertoli, A.; Brennan, A.; Cano, C.; Reeves, H. L.; Newell, D. R.; Golding, B. T.; Miller, D. C.; Griffin, R. J. *Chem. Sci.* **2016**, *7*, 2821–2826.
(7) Schober, M.; Toesch, M.; Knaus, T.; Strohmeier, G. A.; Van Loo, B.; Fuchs, M.; Hollfelder, F.; Macheroux, P.; Faber, K. *Angew. Chem.-Int. Edit.* **2013**, *52*, 3277–3279.
(8) Prechoux, A.; Genicot, S.; Rogniaux, H.; Helbert, W. *Mar. Biotechnol.* **2013**, *15*, 265–274.
(9) Barbeyron, T.; Brillet-Guéguen, L.; Carré, W.; Carrière, C.; Caron, C.; Czjzek, M.; Hoebeke, M.; Michel, G. *PLoS ONE* **2016**, *11*, 1–33.
(10) Toesch, M.; Schober, M.; Faber, K. *Appl. Microbiol. Biot.* **2014**, *98*, 1485–1496.
(11) Yoon, H. Y.; Hong, J.-I. *Anal. Biochem.* **2017**, *526*, 33-38.
(12) Petersen, S. P.; Ahring, B. K. *J. Microbiol. Meth.* **1990**, *12*, 225–230.
(13) Tang, T.-C.; Huang, H.-J. *Anal. Chem.* **1995**, *67*, 2299–2303.
(14) Kolmert, Å.; Wikström, P.; Hallberg, K. B. *J. Microbiol. Meth.* **2000**, *41*, 179–184.
(15) Lundquist, P.; Mårtensson, J.; Sörbo, B.; Ohman, S. *Clin. Chem.* **1980**, *26*, 1178–1181.
(16) van Staden, J. F.; Taljaard, R. E. *Anal. Chim. Acta* **1996**, *331*, 271–280.
(17) Sörbo, B. *Method. Enzymol.* **1987**, *143*, 3–6.
(18) Zhang, M.; Liu, Y.-Q.; Ye, B.-C. *Analyst* **2011**, *136*, 4558–4562.
(19) Gao, Z.; Deng, K.; Wang, X.-D.; Miró, M.; Tang, D. *ACS Appl Mater. Interfaces* **2014**, *6*, 18243-18250.
(20) Zhou, Q.; Lin, Y.; Xu, M.; Gao, Z.; Yang, H.; Tang, D. *Anal. Chem.* **2016**, *88*, 8886-8892.
(21) Lin, Y.; Zhou, Q.; Li, J.; Shu, J.; Qiu, Z.; Lin, Y.; Tang, D. *Anal. Chem.* **2016**, *88*, 1030-1038.
(22) Kameya, M.; Himi, M.; Asano, Y. *Anal.Biochem.* **2014**, *447*, 33-38.
(23) Wei, J.; Tang, Q.-X.; Varlamova, O.; Roche, C.; Lee, R.; Leyh, T. S. *Biochemistry* **2002**, *41*, 8493–8498.
(24) Knaus, T.; Schober, M.; Kepplinger, B.; Faccinelli, M.; Pitzer, J.; Faber, K.; Macheroux, P.; Wagner, U. *FEBS J.* **2012**, *279*, 4374–4384.
(25) White, G. F.; Lillis, V.; Shaw, D. J. *Biochem. J.* **1980**, *187*, 191-196.
(26) Rühmann, B.; Schmid, J.; Sieber, V. *JOVE-J. Vis. Exp.* **2016**, *2016*, 110.
(27) Schober, M.; Knaus, T.; Toesch, M.; Macheroux, P.; Wagner, U.; Faber, K. *Adv. Synth. Catal.* **2012**, *354*, 1737–1742.
(28) Schober, M.; Gadler, P.; Knaus, T.; Kayer, H.; Birner-Grünberger, R.; Gülly, C.; MacHeroux, P.; Wagner, U.; Faber, K. *Org. Lett.* **2011**, *13*, 4296–4299.
(29) Beil, S.; Kehrli, H.; James, P.; Staudenmann, W.; Cook, A. M.; Leisinger, T.; Kertesz, M. A. *Eur. J. Biochem.* **1995**, *229*, 385-394.
(30) Staiano, M.; Pennacchio, A.; Varriale, A.; Capo, A.; Majoli, A.; Capacchione, C.; D'Auria, S. In *Methods in Enzymology*, Richard, B. T.; Carol, A. F., Eds.; Academic Press, 2017, pp 115–131.
(31) Leyh, T. S.; Taylor, J. C.; Markham, G. D. *J. Biol. Chem.* **1988**, *263*, 2409–2416.
(32) Mueller, J. W.; Shafqat, N. *FEBS J.* **2013**, *280*, 3050–3057.
(33) Sun, M.; Leyh, T. S. *Biochemistry* **2006**, *45*, 11304–11311.
(34) Sun, M.; Leyh, T. S. *Biochemistry* **2005**, *44*, 13941–13948.
(35) Karamohamed, S.; Nilsson, J.; Nourizad, K.; Ronaghi, M.; Pettersson, B.; Nyrén, P. *Protein Expres. Purif.* **1999**, *15*, 381–388.
(36) Kameya, M.; Asano, Y. *Enzyme Microb. Tech.* **2014**, *57*, 36–41.
(37) Liu, C.; Wang, R.; Varlamova, O.; Leyh, T. S. *Biochemistry* **1998**, *37*, 3886–3892.
(38) Morais, I. P. A.; Rangel, A. O. S. S.; Souto, M. R. S. *J. AOAC Int.* **2001**, *84*, 59–64.
(39) Tokheim, A. M.; Spannaus-Martin, D. J.; Martin, B. L. *Biometals* **2005**, *18*, 537–540.
(40) Pogorevc, M.; Strauss, U. T.; Riermeier, T.; Faber, K. *Tetrahedron: Asymmetry* **2002**, *13*, 1443–1447.
(41) Chang, B.; Mahoney, R. *Biotechnol. Appl. Bioc.* **1995**, *22*, 203–214.
(42) Zhang JH, C. T., Oldenburg KR. *J. Biomol. Screen.* **1999**, *4*, 67–73.
(43) Gadler, P.; Faber, K. *Eur. J. Org. Chem.* **2007**, *2007*, 5527–5530.

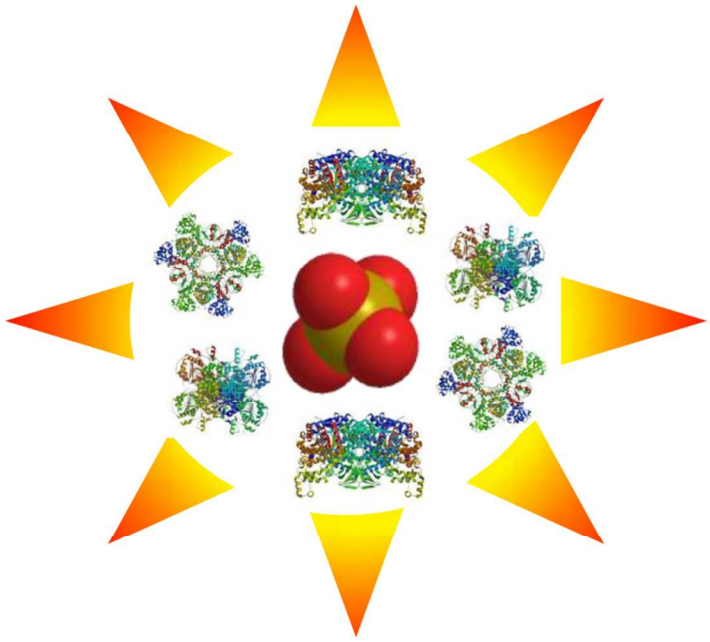

(*For TOC only*)